Energy-Source-Sizing Methodology for Hybrid Fuel Cell Vehicles Based on Statistical Description of Driving Cycles

Alexandre Ravey, *Student Member, IEEE*, Nicolas Watrin, *Student Member, IEEE*, Benjamin Blunier, *Member, IEEE*, David Bouquain, and Abdellatif Miraoui, *Senior Member, IEEE*

***Abstract*—This paper describes a new methodology based on the statistical description of driving cycles to size the energy source of a hybrid vehicle. This methodology is applied to a fuel-cell-based collection truck for very specific driving patterns. Based on experimental data, random driving cycles are then generated, allowing the distribution of the average powers and energies to be computed. The analysis proves that a 20-kW fuel cell stack is sufficient for a 13 000-kg truck. The results show that the fuel cell system could be downsized, compared with classical solutions, where much larger fuel cells are required.**

***Index Terms*—Energy management, fuel cell system, fuzzy logic, hybrid electric vehicle.**

Nomenclature

t	Time (in seconds).
m_v	Vehicle mass (in kilograms).
v	Vehicle speed (in kilometers per hour).
F	Faraday constant (in degrees Celsius).
F_t	Traction force (in Newtons).
F_a	Drag force (in Newtons).
F_r	Rolling friction (in Newtons).
F_g	Gravity force (in Newtons).
F_d	Disturbance force (in Newtons).
$P_v(t)$	Instantaneous vehicle power needed (in watts).
$P(t)$	Instantaneous power (in watts).
A	Front surface (in squared meters).
ρ	Air density (in kilograms per cubic meter).
C_x	Drag coefficient.
C_r	Rolling coefficient.
α	Road slope (in radians).
g	Earth's gravity (in meter per square second).
$\bar{P}$	Average power (in watts).
E	Total energy (in watt-hours).
η_d	Drivetrain efficiency.
T_x	Total time for the x action (in seconds).
P_{H2}	Hydrogen tank pressure (in bars).
V_{H2}	Hydrogen tank volume (in cubic meters).
T	Temperature (in degrees Kelvin).
n_x	Number of moles of x.
n_c	Number of cell.
R	Ideal gas constant (in joules per mole Kelvin).
M_H	Hydrogen molar mass (in grams per mole).
m_{H2}	Hydrogen mass (in grams).
LHV	Lower heating value (in megajoules per kilogram).
η_{FCS}	Fuel cell hydrogen efficiency.
$soc(t)$	Battery state of charge.
soc_{init}	Initial battery state of charge.
C_{init}	Initial capacity (in watt-hours).

Manuscript received November 1, 2010; revised March 10, 2011; accepted May 2, 2011. Date of publication June 2, 2011; date of current version December 9, 2011. The review of this paper was coordinated by Prof. A. Emadi.

The authors are with the University of Technology of Belfort-Montbéliard, 90000 Belfort, France (e-mail: alexandre.ravey@utbm.fr; nicolas.watrin@utbm.fr; benjamin.blunier@utbm.fr; david.bouquain@utbm.fr; abdellatif.miraoui@utbm.fr).

Color versions of one or more of the figures in this paper are available online at http://ieeexplore.ieee.org.

Digital Object Identifier 10.1109/TVT.2011.2158567

I. Introduction

In TRANSPORT applications, proton exchange membrane fuel cells appear to be suitable in some cases and particularly niche markets such as vehicle fleets as they provide very good tank-to-wheel efficiency, compared with internal combustion engines [1], [2]. In cities, hydrogen may lead to zero-emission vehicles. However, even if the tank-to-wheel efficiency is good, the well-to-tank efficiency has to be carefully studied to have the most clean and environmentally friendly hydrogen production [1], [3].

In this paper, only fuel cells are considered for transport applications. The hydrogen is stored onboard and is supplied by a hydrogen infrastructure. In other kinds of applications, hydrogen can be produced with reformate produced from natural gas, liquefied petroleum gas, or renewable liquid fuels (i.e., distributed stationary power generation). For electronic devices in small equipment, methanol and, sometimes, hydrogen are the fuels of choice in fuel cell systems.

The technical challenges and objectives for fuel cell systems in transportation applications are given by the Department of Energy [4]–[8]. The major challenges are cost and durability. To become competitive with internal combustion engines ($25–$35 per kilowatt), the price of the fuel cell system, including all the subsystems, has to be reduced to about $35 per kilowatt.[1] The durability with cycling of the system should meet the requirements of automotive applications and extend their

[1] 2015 targets. The 2010 target is $45 per kilowatt.

lifetime up to 5000 h[2] (about 240 000 km). The fuel cell system should be able to start and work with temperatures ranging from -40 °C to $+40$ °C. In these temperature conditions, the start-up time to 50% of the rated power (80 kW) has to be as small as possible: 30 s at -20 °C and 5 s at $+20$ °C.

On the other hand, the size and weight of current fuel cell systems have to be drastically reduced to meet the automotive compactness requirements, which apply to both the fuel cell stack and auxiliary components such as compressors, gas expanders, humidifiers, pumps, sensors, and hydrogen storage. The specific power and the power density requirements are 650 W/kg and 650 W/l, respectively, for the fuel cell system and 2000 W/kg and 2000 W/l, respectively, for the stack itself.

In transport applications, the transient response of the stack is also a key issue and mainly depends on the air supply system: the transient response from 10% to 90% of the maximum power should be lower than 1 s.

The aim of this paper is to show how a hybrid power system can help reach these targets, particularly for city vehicles such as collection trucks, which have very special driving mission profiles that depend on many parameters. It shows that, on the one hand, a peaking power source (PPS) can improve the system performance and fuel economy, and on the other hand, the PPS allows the fuel cell system to be drastically downsized and reduces, at the same time, the price of the fuel cell system, which is the most expensive part of the overall system.

To do this, we are working on garbage truck driving cycle profiles, which are very different from those that can be found in the literature, where very specific cycles [9]–[11] or standard driving cycles are commonly used [2], [12], [13]. Such standard driving cycles as the urban dynamometer driving schedule or standardized CYCles (CYC) represent different road constraints, speeds, and road slopes, and are used in most publications to size electrical power trains [2], [14]. However, these standard cycles only account for some precise conditions and may not always be representative of real-world driving conditions. Numerous variables, e.g., the number of starts, pause durations, etc., can vary much from one driver to another. This led us to create our own cycles based on real cycles measured on a garbage truck. A driving cycle generator computes many different profiles and tests them on a garbage truck similar to that used to measure the cycle.

This paper starts by presenting the collection truck and its driving mission profiles. The following gives the specific methodology based on random cycle generation to size both the fuel cell stack and battery pack. In the last part, a fuzzy logic controller is implemented in the vehicle to validate the proposed methodology. Finally, conclusions are drawn based on the simulation results.

In a previous paper [15], the authors introduced a methodology based only on simulation without real cycles and the associated control. This paper presents an improvement of the previously introduced methodology where real data are used, and the design is validated, together with a proper energy management strategy based on a fuzzy logic controller.

[2]20 000 h in steady-state conditions.

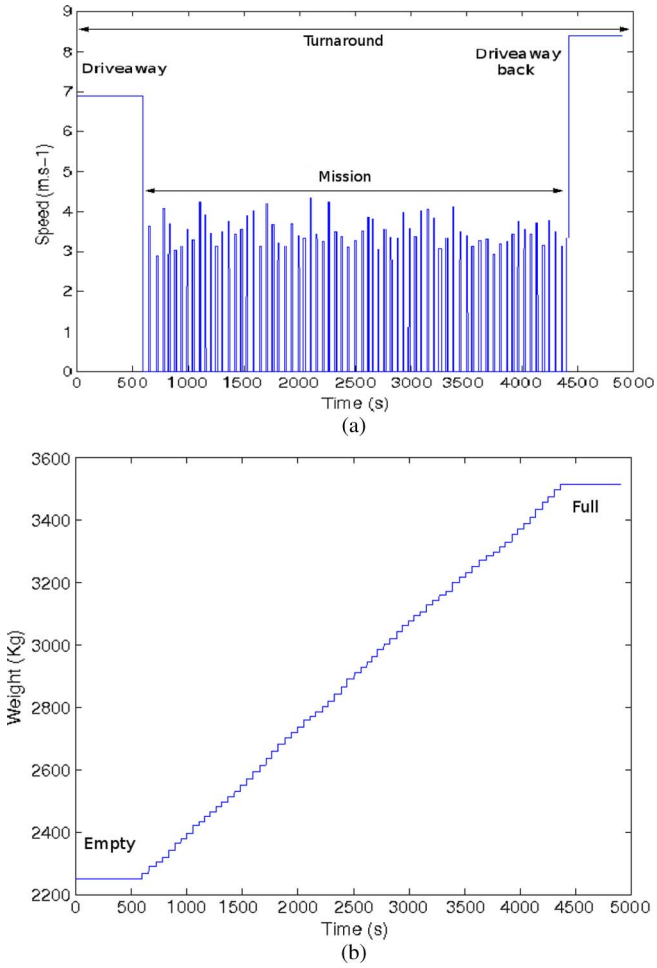

Fig. 1. Vehicle speed and mass profiles for one turnaround. (a) Speed profile. (b) Truck weight profile.

II. Random Driving Cycle Generation Using Statistical Description of the Vehicle's Characteristics Based on Real Measures

For a collection truck, standardized driving cycles such as the standardized European driving cycle (EEC Directive 90/C81/01) cannot be used since a collection truck has very special driving mission profiles, depending on many parameters, such as driveaway distance, collection truck capacity, distance between the houses, working speed, and driveaway speed (cruising speed). Thus, an adapted and representative driving cycle has to be used to properly size the energy source, i.e., a fuel cell system (stack power and hydrogen tank) in this case. The methodology is based on random driving cycle generation and statistical distribution of many parameters.

The consumption of the nonpropulsion loads (e.g., garbage disposer) is not considered in this paper as the considered truck does not have a garbage compacter. If such auxiliaries are considered, they should not be neglected as the power might be quite high when the truck is full.

A. Driving Cycle Definition

This study is based on data collected on a real collection truck during its work time. As shown in Fig. 1(a), the presented driving cycle describes the trip between the garbage center

(driveaway) where the truck starts empty, the collecting phase (mission), and the return when the truck is full (driveaway back). During this trip (turnaround), several parameters are randomly chosen based on real statistical data, which may differ between cities and are given as follows:

1) *driveaway distance:* distance between the garbage center and the first house;
2) *driveaway speed:* drive speed from the center to the first house;
3) *working speed:* drive speed from one house to another;
4) *working distance:* distance between two houses;
5) *collection time:* time to collect the garbage of one house;
6) *garbage weight:* weight of the garbage of one house that needs to be collected in the truck;
7) *road slope.*

All of these parameters are changing at each step of the mission.

B. Statistical Distribution Definition Extract From an Experimental Driving Cycle

The aim of the first part of this study is to define each parameter from measured driving profile statistical distributions. These parameters will then used to generate random driving cycles. Theses driving profiles are obtained from several real turnaround of a garbage collector truck in the city of Belfort, France. These cycles have been measured using a Global Positioning System (GPS) cell, together with accelerometers, i.e., the BOXV74-PRO from the ISAAC company. Several parameters are collected in real time while the truck is driving, such as the following:

1) *speed:* the speed of the vehicle measured by the GPS;
2) *acceleration:* the acceleration of the vehicle measured by the embedded accelerometer of the GPS cell;
3) *GPS altitude:* the altitude of the vehicle measured by the GPS (used to determine the slope between two measure points);
4) *time:* the time (used to define the driving cycle (speed versus time) and the time when the vehicle is at zero speed or stopped times).

Moreover, the garbage is weighted to determine the statistical distribution of the garbage weights.

All parameters are then analyzed to determine the distributions: Fig. 2(a)–(c) shows the working speeds, times at zero speed (stopped times), and acceleration distributions, respectively.

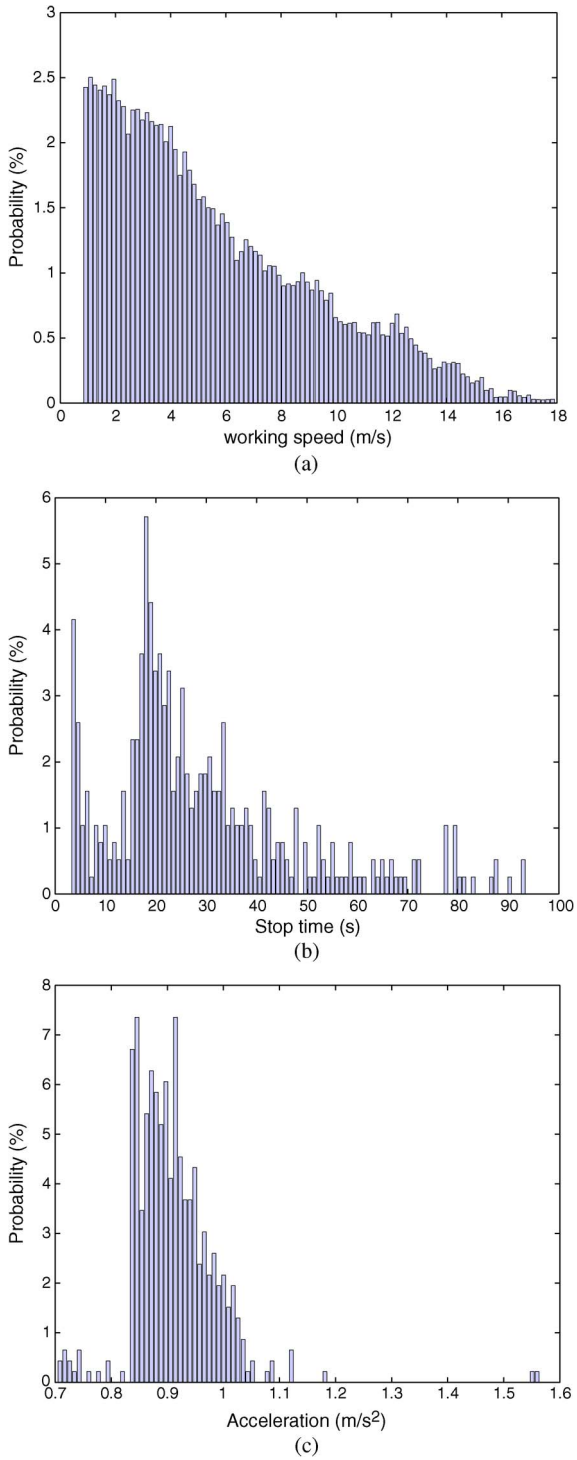

Fig. 2. Statistical distributions. (a) Working speed distribution. (b) Stopped time distribution. (c) Acceleration distribution.

C. Driving Cycle Generation

Based on real statistical distributions of parameters, it is possible, at each time step of the simulation, to randomly select a set of parameters to generate a driving cycle that will be statistically representative of real driving patterns.

The end of the cycle depends on whether the truck is full or not. A complete turnaround cycle is described here.

1) The empty truck goes out of the center: The driveaway distance, driveaway speed, and slope values are randomly picked up.
2) The truck collects the first bin: The garbage weight and collection time values are randomly picked up.
3) If the truck is not full, the working distance, working speed, and slope values are randomly picked up, and the cycle continues from step 2 until the truck is full.
4) When the truck is full, the driveaway distance, driveway speed, and slope values are randomly picked up.

The driving cycle can be obtained by combining all the preceding steps. A graphical representation of the speed profile

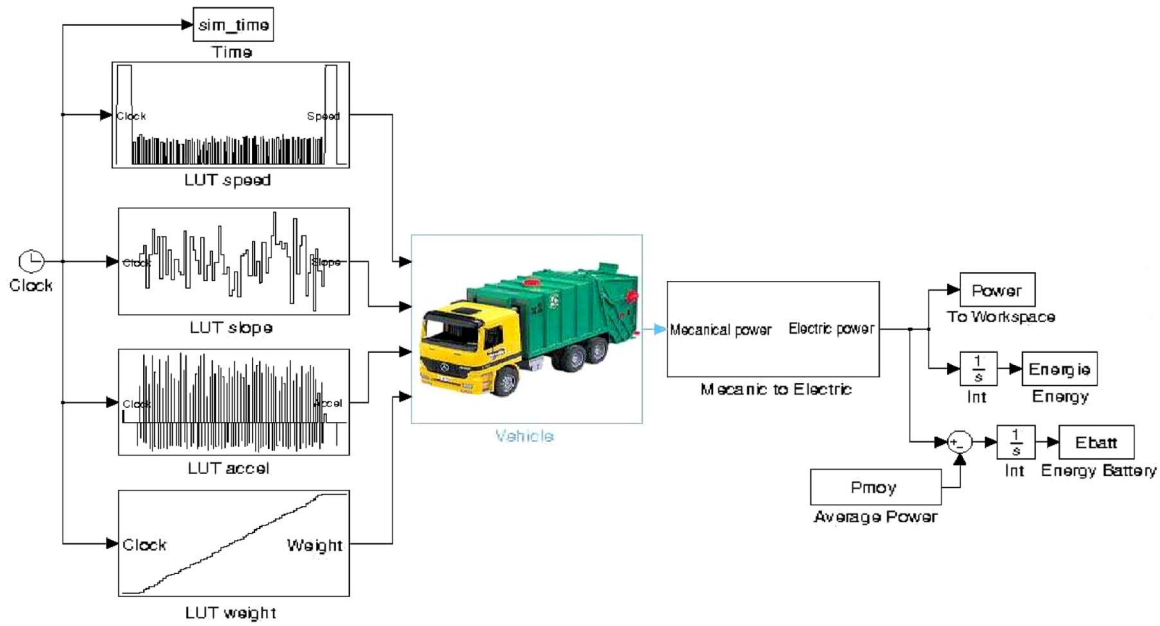

Fig. 3. Simulink vehicle's model.

for a generated driving cycles is shown in Fig. 1(a), and the corresponding time evolution of the vehicle weight is given in Fig. 1(b).

During the simulation, 5000 driving cycles are generated, and each of them is analyzed to determine the average power, turnaround energy, time of one turnaround, and other useful quantities. The overall results give the output distributions (average power, turnaround time, etc.) based on the input distributions. The result distributions can be analyzed to correctly size the fuel cell stack and the PPS.

III. Simulation of 5000 Generated Driving Cycles Based on the Vehicle's Model

A. Vehicle's Model

Newton's second law is used to determine the instantaneous power demand of the vehicle at each step of the simulation [16]

$$m_v(t)\,\frac{d}{dt}\,v(t) = F_t(t) - (F_a(t) + F_r(t) + F_g(t) + F_d(t)) \quad (1)$$

$$P_v(t) = v\,F_t(t) \quad (2)$$

where

$$F_t(t) = m_v(t)\frac{d}{dt}v(t) + F_a(t) + F_r(t) + F_g(t) + F_d(t) \quad (3)$$

where F_a is the drag force, F_r is the rolling friction, F_g is the force caused by gravity when driving on nonhorizontal roads, F_d is the disturbance force that summarizes all other effects, and F_t is the traction force, which depends on speed and acceleration

$$F_a = \frac{1}{2}\,\rho\,A\,C_x\,v^2 \quad (4)$$

$$F_r = m_v(t)\,C_r\,g\,\cos(\alpha) \quad (5)$$

$$F_g = m_v(t)\,g\,\sin(\alpha) \quad (6)$$

where $m_v(t)$ is the vehicle mass in kilograms. It has to be noted that, in this case, $m_v(t)$ depends on time. α is the road slope expressed in radians. The vehicle's model in Matlab/Simulink is shown in Fig. 3. The model parameters are the speed, slope, acceleration, and weight of truck for each step of the simulation. The simulated truck has the following characteristics:

1) empty weight: 13 000 kg;
2) mass when fully loaded: 19 000 kg;
3) front surface (A): 7 m^2;
4) drag coefficient (C_x): 0.8;
5) rolling coefficient (C_r): 0.015;
6) drivetrain efficiency: 0.72.

B. Simulation

The sequential algorithm used to run the simulation is shown in Fig. 4. Each generated driving cycle is simulated using the vehicle model and the instantaneous power $P(t)$ at each time step. Thus, the average power $\bar{P}$ and the total energy E at the end of each cycle can be computed using

$$P(t) = \frac{P_v(t)}{\eta_d} \quad (7)$$

$$\bar{P} = \frac{1}{T_{\text{turnaround}}} \int_0^{T_{\text{turnaround}}} P(t)\,dt \quad (8)$$

$$E = \bar{P} \cdot T_{\text{turnaround}} \quad (9)$$

respectively, where η_d is the drivetrain efficiency, and $T_{\text{turnaround}}$ is the total time of the turnaround including all stop, working, and driveaway times.

As each turnaround driving profile is different, the average power and any other quantities such as the total time ($T_{\text{turnaround}}$) for each turnaround will vary. For example, Fig. 5 shows the statistical distribution of the total time of a turnaround.

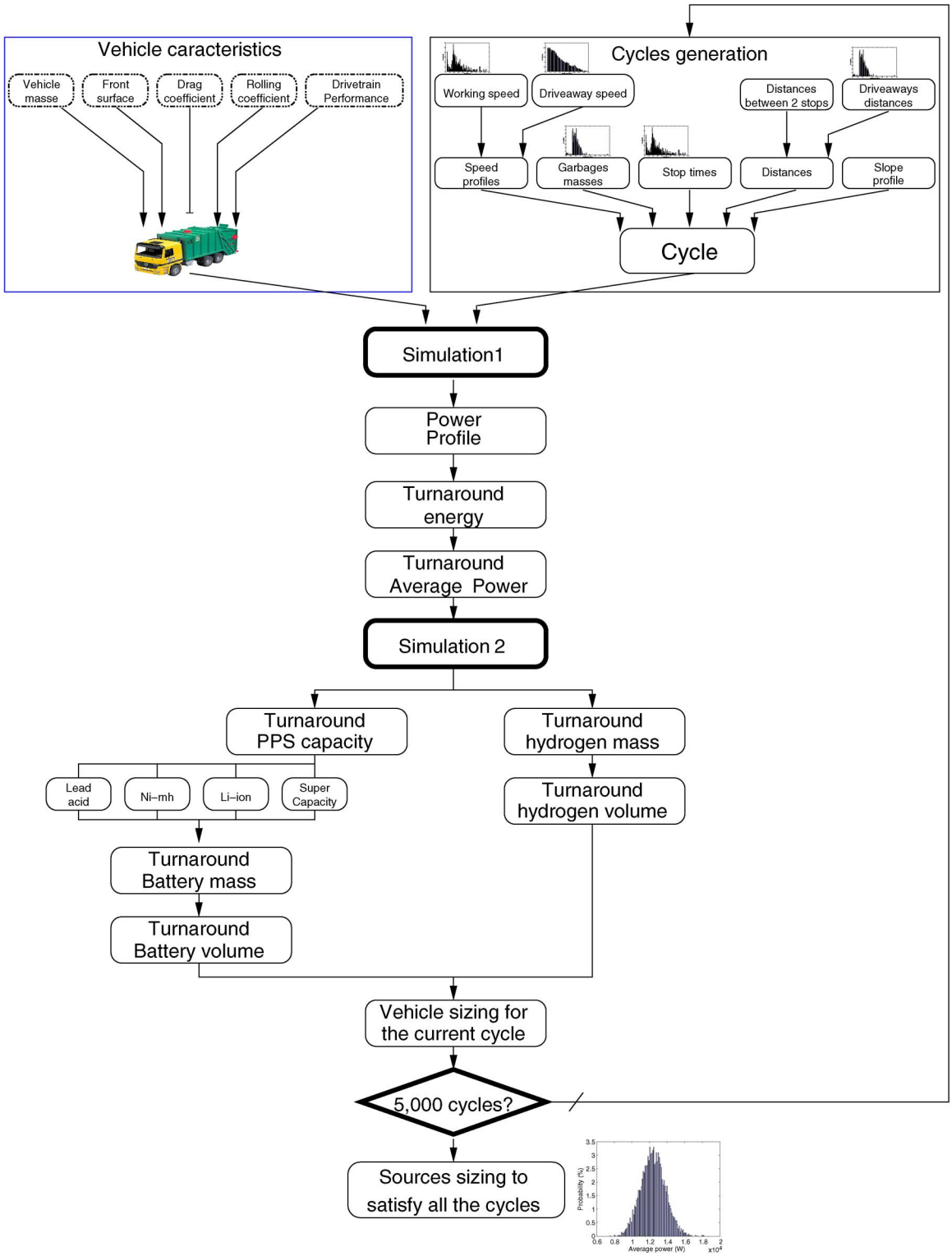

Fig. 4. Algorithm flowchart.

After the first simulation, a second simulation is run using the average power obtained in the first simulation with the same driving profile. The second simulation determines the energy profile along the time of PPS source (battery)

$$E_{\text{battery}}(t) = \int P_{\text{current}}(t) - \bar{P}(t)\, dt \tag{10}$$

and its corresponding capacity

$$C_{\text{battery}}\,(\text{Wh}) = E_{\text{battery max}} - E_{\text{battery min}}. \tag{11}$$

The results obtained from these two simulations are used to size the energy storage sources (fuel cell power, hydrogen mass, battery power, and energy capacity).

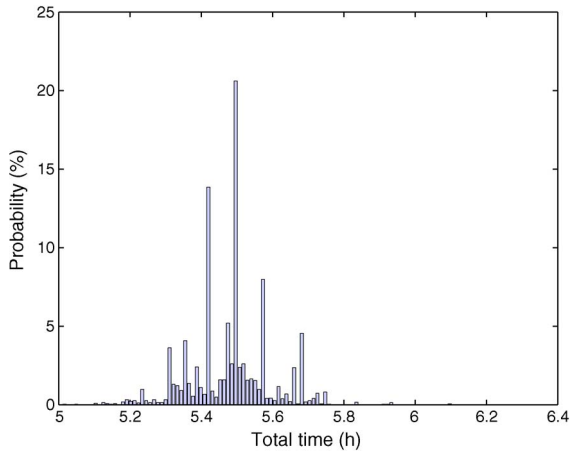

Fig. 5. Total time distribution ($T_{\mathrm{turnaround}}$).

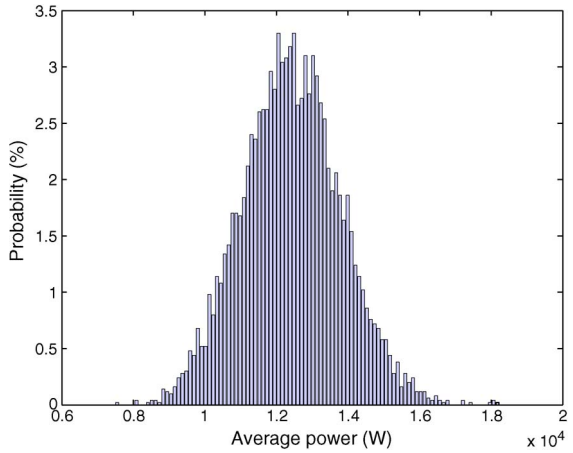

Fig. 6. Turnaround average power distribution with 60% breaking energy recovery.

IV. Fuel Cell Stack Power Needs

A. Average Power and Energy Distributions

After a simulation of 5000 turnarounds, the average power distribution is computed and shown in Fig. 6. It can be clearly seen that the distribution of the average powers is a normal distribution centered on 13 kW.

The high number of simulation (5000) has been chosen to have more precise results, keeping an acceptable simulation time (about 25 min for 5000 simulations). However, it has been shown that, from a number of 1000 simulations, the results are acceptable.

The average power distribution shows that the maximum average power required for one turnaround does not exceed 18 kW. A 20-kW fuel cell stack will satisfy 100% of the simulated cases based on the chosen parameters. These results allow the fuel cell stack and the hydrogen quantity to be chosen, depending on how much turnarounds are planed for one day. Moreover, if the hydrogen infrastructure is equipped with a fast recharge station, the hydrogen tank does not need to be sized for the needs of one day but only for a few turnarounds. The hydrogen storage tank sizing methodology will be given in Section VI-C.

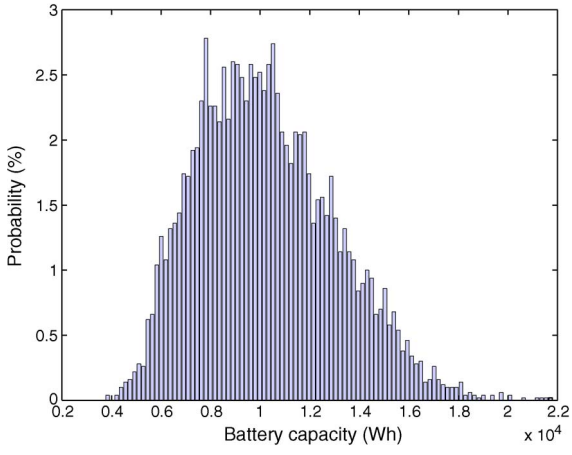

Fig. 7. Battery capacity assuming 60% breaking energy recovery.

Once the fuel cell power (*i.e., average power*) is computed, it is assumed that the fuel cell always outputs the average power (also during stop phases) when the truck is collecting garbage. This average power can be subtracted from the instantaneous power to determine the power needed by the PPS [17].

V. Peaking Power Source Energy Needs

Once the average power is determined, a second simulation is run to determine the energy (10) and capacity (11) of the second power source by integrating its power. The results are given in Fig. 7. It is assumed that the truck is not a plug-in vehicle: The initial and final battery's states of charges must be the same. The fuel cell recharges the battery when the power needed by the vehicle is below the average power (i.e., fuel cell power).

The battery capacity has been calculated based on the battery state of charge (SoC) constraints: Depending on the technology, the SoC should be between a minimum (15%–20% for lithium-based batteries and lead-acid batteries) and a maximum (100%). The battery capacity is calculated based on the fact that the fuel cell constantly runs at the average power of the driving cycle, and the battery gives or absorbs the remaining power. These results show that the maximum battery capacity does not exceed 23 kWh. A battery pack with 25 kWh will satisfy 100% of the simulated cases based on the chosen parameters.

VI. Practical Sizing of Both Energy Sources

A. Fuel Cell and Battery Capacity for Several Braking Recovery Rate

Table I shows the average power of the vehicle and the battery capacity needed for the truck for several braking recovery rates. For this study, due to repeated starts and stops, it is assumed that the recovery of braking energy rate is 60% [18].

B. Size of the Battery Pack

Table II shows the mass and volume of different PPS technologies based on the specific power and energy density given in [19]. This table is based on an energy recovery of 60%.

TABLE I
FUEL CELL AND BATTERY CAPACITY FOR SEVERAL BRAKING RECOVERY RATES

Braking recovery	Average power (W)	Battery capacity (Wh)
0 %	21,600	24,800
30 %	19,900	23,100
60 %	18,300	21,900
100 %	16,400	20,600

TABLE II
SIZE OF THE PPS FOR SEVERAL TECHNOLOGIES ASSUMING A 60% ENERGY RECOVERY DURING BRAKING PHASES

Type	Mass (kg)	Volume (l)
Lead-acid	2,500	1,150
Nickel-metal	600	175
Lithium-ion	500	175
Ultracapacitors	2,000	1,000,000

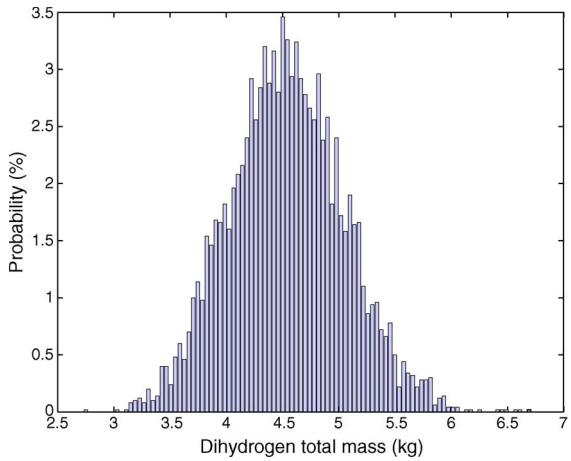

Fig. 8. Hydrogen mass needed for one cycle with 60% breaking energy recovery.

Due to their very low energy density (10 Wh/kg) [20], it is shown that the ultracapacitors are not suitable for this application. However, a triple hybrid vehicle including fuel cell (low dynamics, low power, and overall energy), battery (medium dynamics, medium power, and medium energy), and ultracapacitors (high dynamics, high power, and low energy) could be interesting, but this would increase at the same time as the vehicle complexity. For this reason, this solution is not investigated.

C. Size of the Hydrogen Tank

Once the fuel cell power is known, the quantity of hydrogen can be calculated to satisfy all the cycles. The mass and volume of the hydrogen onboard are deduced from the energy provided by the fuel cells. Currently, most of the hydrogen tanks are pressurized to 300 bar, with a minimum pressure of 30 bar (i.e., empty tank). Knowing the power of the fuel cell and the duration of one turnaround, it is possible to calculate the energy needed. The distribution mass of hydrogen is then determined (see Fig. 8). The number of moles $n_{\text{turnaround}}$ and, subsequently, the volume of hydrogen can be deduced from the mass, as shown in Fig. 9.

To ensure a proper hydrogen supply of the fuel cell, the pressure in the tank has to be higher than 30 bar for a 300-bar tank. Consequently, all the hydrogen in the tank cannot be used,

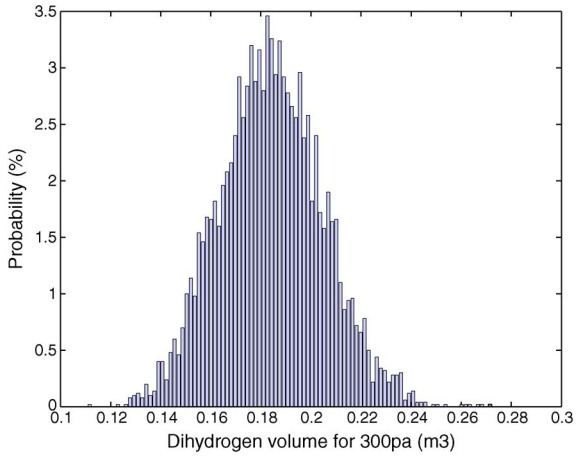

Fig. 9. Hydrogen volume needed for one cycle with a 300-bar pressurized tank and 60% breaking recovery.

and an extra amount of hydrogen n_{extra} must be added. This extra amount must be taken into account to compute the final volume of the hydrogen tank.

From the ideal gas law, we have

$$P_{\text{H}_2} \cdot V_{\text{H}_2} = n_{\text{H}_2} \cdot R \cdot T \tag{12}$$

where

$$m_{\text{H}_2} = \frac{E}{LHV \cdot \eta_{\text{FCS}}} \tag{13}$$

$$n_{\text{H}_2} = \frac{m_{\text{H}_2}}{2 \cdot M_H} \tag{14}$$

$$n_{\text{H}_2} = n_{\text{turnaround}} + n_{\text{extra}}. \tag{15}$$

LHV is the lower heating value of hydrogen ($LHV = 120.1$ MJ/kg), η_{FCS} is the fuel cell hydrogen efficiency, and M_H is the hydrogen molar mass.

Combining (12) and (15) gives

$$P_{\text{H}_2} \cdot V_{\text{H}_2} = (n_{\text{turnaround}} + n_{\text{extra}}) \cdot R \cdot T. \tag{16}$$

The pressure at the end of the turnaround is P_{extra}; therefore, n_{extra} is given by

$$n_{\text{extra}} = \frac{P_{\text{extra}} \cdot V_{\text{H}_2}}{R \cdot T}. \tag{17}$$

Each hydrogen volume can be obtained using (17) with (16)

$$n_{\text{turnaround}} + n_{\text{extra}} = \frac{P_{\text{H}_2} \cdot V_{\text{H}_2}}{R \cdot T} \tag{18}$$

$$n_{\text{turnaround}} = \frac{P_{\text{H}_2} \cdot V_{\text{H}_2}}{R \cdot T} - \frac{P_{\text{extra}} \cdot V_{\text{H}_2}}{R \cdot T} \tag{19}$$

$$n_{\text{turnaround}} = \frac{(P_{\text{H}_2} - P_{\text{extra}}) \cdot V_{\text{H}_2}}{R \cdot T} \tag{20}$$

$$V_{\text{H}_2} = \frac{n_{\text{turnaround}} \cdot R \cdot T}{(P_{\text{H}_2} - P_{\text{extra}})} \tag{21}$$

where P_{H_2} is the hydrogen tank pressure in Pascal, R is the ideal gas constant ($R = 8.314$ J $\cdot$ mol^{-1} $\cdot$ K^{-1}), T is the tank temperature in degrees Kelvin, n_{H_2} is the number of moles of hydrogen for one turnaround, and n_{extra} is the moles of hydrogen at the end of a turnaround.

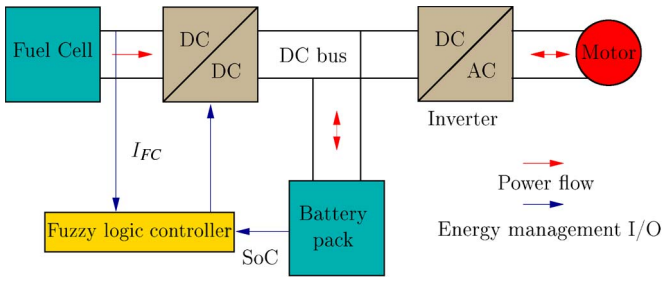

Fig. 10. Drivetrain topology including energy management system.

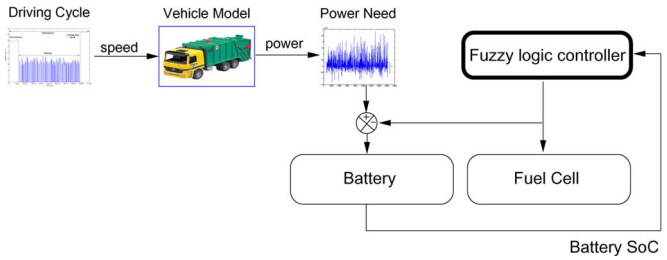

Fig. 11. Fuzzy logic controller principle.

VII. Validation of the Design Using a Fuzzy-Logic-Based Controller

A. Architecture

Fig. 10 shows the drivetrain topology including the energy management system. The fuzzy controller will set the fuel cell current due to its associated dc/dc converter based on the battery SoC.

B. Fuel Cell Model

The fuel cell is used as the primary source of energy, and the objective of the fuzzy rules is to minimize the hydrogen consumption given by

$$m_{H2} = \int_0^t \frac{M_{H_2}\, n_c}{2\, F} I_{\mathrm{FC}}(t)\, dt \tag{22}$$

where m_{H_2} is the hydrogen mass, M_{H_2} is the hydrogen molar mass, n_c is the number of cells, I_{FC} is the fuel cell current, and F is the Faraday constant (96 487 C). Fuel cell current I_{FC} permits the fuel cell power to be computed based on a simple fuel cell stack polarization curve.

C. Battery Model

The battery model is based on a simple current integration to know the battery SoC at each instant time (23). The battery voltage is not considered in this model as the objective of the simulation is to obtain the energy to be stored in the battery for a turnaround

$$\mathrm{SoC}(t) = \mathrm{SoC}_{\mathrm{init}} - \frac{1}{C_{\mathrm{init}}} \cdot \Sigma i(t) \cdot \Delta t. \tag{23}$$

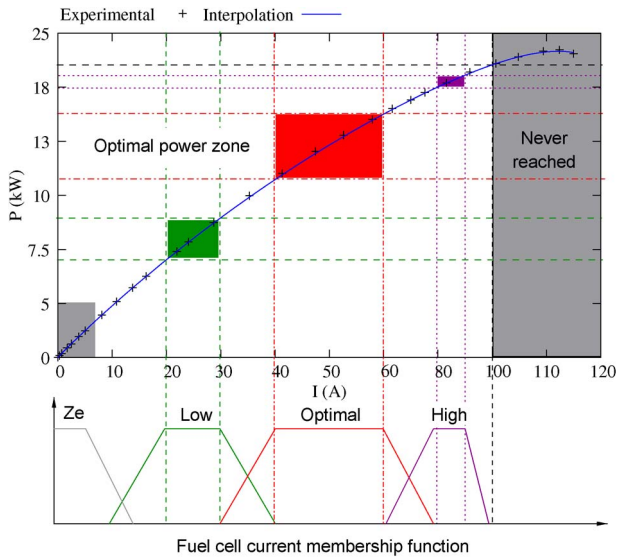

Fig. 12. Working zones of the fuel cell system.

TABLE III
Battery SoC Membership Function Parameters [21]

Description	Notation	SoC Value
Emergency case	SoC_{limit}	0.1
SoC is considered to be low	$SoC_{\mathrm{low_{min}}}$	0.2
	$SoC_{\mathrm{low_{max}}}$	0.5
SoC is considered to be good (optimal)	$SoC_{\mathrm{good_{min}}}$	0.6
	$SoC_{\mathrm{good_{max}}}$	0.85
SoC is considered to be high (the system can work in charge depleting mode in this case : only the battery is working)	$SoC_{\mathrm{high_{min}}}$	0.95
	$SoC_{\mathrm{high_{max}}}$	1

TABLE IV
Fuel Cell Current Membership Function Parameters [21]

Description	Notation	Current (A)
Fuel cell maximum current allowed	$FC_{\mathrm{current_{max}}}$	130
Fuel cell current is considered to be low	$FC_{\mathrm{current\_low_{min}}}$	50
	$FC_{\mathrm{current\_low_{max}}}$	80
Fuel cell current for which the fuel cell has been designed (corresponding to the average power of the load)	$FC_{\mathrm{current\_opt_{min}}}$	90
	$FC_{\mathrm{current\_opt_{max}}}$	110
Fuel cell current is considered to be high (used in emergency cases when the battery SoC is too low)	$FC_{\mathrm{current\_high_{min}}}$	112
	$FC_{\mathrm{current\_high_{max}}}$	120

D. Fuzzy Logic Controller Presentation

In this part of the study, a fuzzy logic controller will be implemented on the designed vehicle to verify the goodness of the sizing.

The control strategy has to take into account four constraints [21].

1) The fuel cell dynamics and voltage cycling (low voltages) are limited to increase its lifetime. Ideally, the fuel cell should work at a constant power corresponding, in this case, to the driving cycle average power.

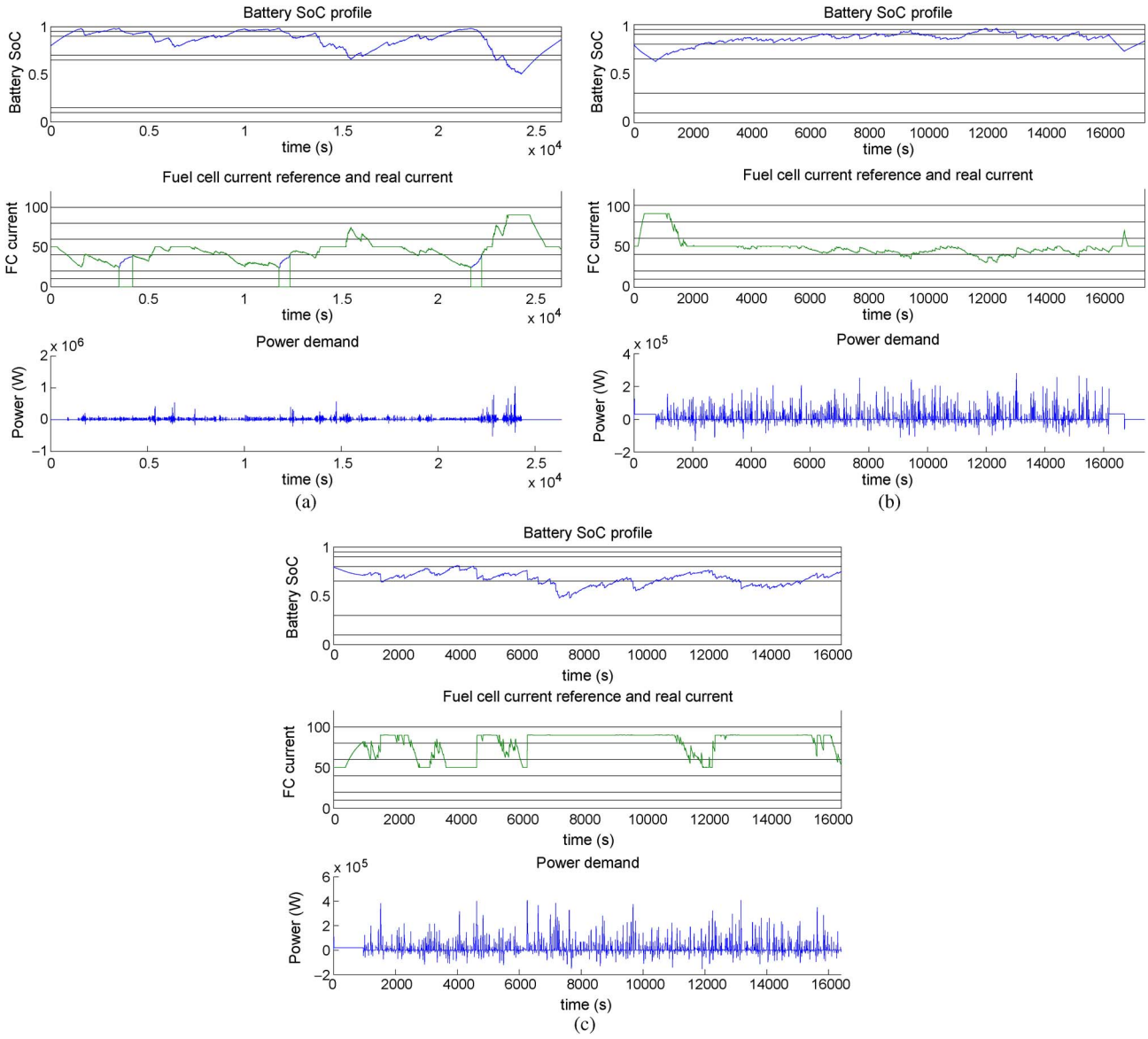

Fig. 13. Battery pack state of charge and fuel cell current. (a) Real driving cycle. (b) Randomly generated driving cycle. (c) Worst-case scenario of generated driving cycle.

2) The fuel cell should work around its optimal working points, where its efficiency is the highest. The fuel cell has been designed for that in the previous sections.
3) The battery SoC is maintained in a given marge and limits the cycling.
4) The energy is recovered during braking phases.

Fig. 11 shows the implementation of the fuzzy controller. The input of the controller is the SoC of the battery pack. The parameters of the fuzzy controller are tunable by the user and are represented by trapezoidal functions, as shown in Fig. 12.

The parameters of the battery SoC management and fuel cell current are given in Tables III and IV, respectively.

The fuel cell nominal power is 20 kW. According to the analyses previously done (see Fig. 6), the most probable average power of the fuel cell is 13 kW. That is why the optimal zone of the fuel cell has to be about 13 kW.

The implemented rules are given here [21].

1) If (SoC is too low), then (fuel cell current (IFC) is too high).
2) If (SoC is low), then (IFC is high).
3) If (SoC is good), then (IFC is opt).
4) If (SoC is high), then (IFC is low).

E. Control of the Designed Vehicle on Two Driving Cycles

Three simulations are run.

1) We run a simulation with a real driving cycle. Note that this driving cycle has not been used to determine the statistical distributions.
2) We run simulation with a randomly generated driving cycle based on the statistical distributions.
3) We run simulation with the worst scenario case where the average power is the maximum of the statistical distributions.

For both simulations (Fig. 13), it is assumed that the initial SoC is 80%. This will show that, if the vehicle can start with a SoC different from 100%, the controller can manage the recharge of the battery SoC at the end of the cycle.

TABLE V
HYDROGEN CONSUMPTION

Type of driving cycle	Average power (kW)	Hydrogen consumption (g)
Real	14,3	3800
Random	9,1	3600
Worst case scenario	18,1	4600

During the driveaway, the energy consumption is important (i.e., the instantaneous power demand is higher than the fuel cell power), the speed and the driving time are relatively high. The fuel cell operates at its optimal power, and the battery significantly discharges.

Once the driveaway ends, when the energy consumption is lower, the fuel cell recharges the battery and works beyond its optimal zone, depending on the SoC of the battery pack.

The charge of the power source therefore rapidly rises at the beginning of the collecting phase. During that phase, the fuel cell works most of the time in its optimal zone.

In some cases, the battery can provide all the required power as its SoC is high [see Fig. 13(a)]; the fuel cell can be turned off for a long time.

Finally, when the truck is back at the center after a driveaway back, the fuel cell continues to operate to recharge the battery until its optimal SoC is reached. This operation could be avoided by plugging the vehicle to the grid, which would reduce the vehicle's overall fuel consumption.

Table V shows the hydrogen consumption along the real cycle, the randomly generated cycle, and the worst-case scenario of generated driving cycle. The hydrogen consumption with the fuzzy controller is about 4 kg, which corresponds to the mass of hydrogen given in Fig. 8.

We can conclude that the fuzzy controller reaches its objectives: the fuel cell works around it optimal power without a high dynamic, and the battery SoC is kept, most of the time, in the optimal SoC window defined by the user.

VIII. CONCLUSION

This paper has described a new methodology to size the energy source of a hybrid vehicle based on the statistical description of driving cycles. This methodology has been applied to a fuel-cell-based collecting truck for which the driving pattern is very specific but could also be adapted for other types of energy sources, such as internal combustion engines. Random driving cycles have been generated, allowing the distribution of the average powers and energies to be computed. The analysis has shown that, even for a 13 000-kg truck, a 20-kW fuel cell stack is sufficient, allowing the fuel cell system to be downsized, compared with classical solutions using several tens of kilowatts of fuel cell systems. A fuzzy logic controller has been implemented to verify the design. This fuzzy logic control has been shown to improve the efficiency of the system by concentrating on the region of operation in the best performance range and minimizing the shutdown and overcurrent conditions, improving, at the same time, the lifetime of the fuel cell system.

REFERENCES

[1] B. Blunier and A. Miraoui, *20 Questions Sur la Pile à Combustible*, Paris, France: Technip, 2008 (in French).

[2] R. Joumard, M. André, R. Vidon, P. Tassel, and C. Pruvost, "Influence of driving cycles on unit emissions from passenger cars," *Atmos. Environ.*, vol. 34, no. 27, pp. 4621–4628, 2000.

[3] B. Blunier and A. Miraoui, *Piles à combustible, Principe, modélisation et applications avec exercices et problèmes corrigés*. Paris, France: Ellipses, 2007, ser. Technosup (in French).

[4] Dept. Energy, Hydrogen, Fuel Cells and Infrastructure Technologies Program, Multi-Year Research, Development and Demonstration Plan, May 2007. [Online]. Available: www1.eere.energy.gov/hydrogenandfuelcells/mypp/

[5] B. Blunier and A. Miraoui, "Proton exchange membrane fuel cell air management in automotive applications," *J. Fuel Cell Sci. Technol.*, vol. 7, no. 4, pp. 041007, Aug. 2010. [Online]. Available: http://link.aip.org/link/?FCT/7/041007/1

[6] J. T. Pukrushpan, A. G. Stefanopoulou, and H. Peng, "Control of Fuel Cell Power Systems: Principle, Modeling Analysis and Feedback Design," in *Advances in Industrial Control*. London, U.K.: Springer UK, 2004.

[7] B. Blunier, D. Bouquain, and A. Miraoui, "Fuel cells, energy management using fuel cells and supercapacitors," in *Alternative Propulsion Systems for Automobiles*. Böblingen, Germany: Expert Verlag, 2008, pp. 97–116.

[8] B. Blunier and A. Miraoui, "Air management in pem fuel cell: State-of-the-art and prospectives," in *Proc. ACEMP, Electromotion, IEEE-PES-MSC*, Sep. 2007, pp. 245–253.

[9] D. B. Q. Cai, D. J. L. Brett, N. Brandona, and D. Browning, "A sizing-design methodology for hybrid fuel cell power systems and its application to an unmanned underwater vehicle," *J. Power Sources*, vol. 195, no. 19, pp. 6559–6569, Oct. 2010.

[10] C. R. Akli, X. Roboam, and A. Jeunesse, "Energy management and sizing of a hybrid locomotive," in *Proc. Power Electron. Appl.*, 2007, pp. 1–10.

[11] S. Fish and T. B. Savoie, "Simulation-based optimal sizing of hybrid electric vehicle components for specific combat missions," *IEEE Trans. Magn.*, vol. 37, no. 1, pp. 485–488, Jan. 2001.

[12] J. R. Kenworthy, "Driving cycles, urban from and transport energy," Ph.D. dissertation, Murdoch Univ., Perth, Australia, 1986.

[13] T. Y. Z. Liang, Z. Xin, and Z. Xinn, "Intelligent energy management based on the driving cycle sensitivity identification using SVM," in *Proc. 2nd Int. Symp. Comput. Intell. Des.*, 2009, pp. 513–516.

[14] M. Jain, C. Desai, N. Kharma, and S. Williamson, "Optimal powertrain component sizing of a fuel cell plug-in hybrid electric vehicle using multi-objective genetic algorithm," in *Proc. 35th Annu. IEEE IECON*, pp. 3741–3746.

[15] A. Ravey, N. Watrin, B. Blunier, and A. Miraoui, "Energy sources sizing for hybrid fuel cell vehicles based on statistical description of driving cycles," in *Proc. IEEE VPPC*, 2010, pp. 1–6.

[16] L. Guzzella and A. Sciarretta, *Vehicle Propulsion Systems, Introdution to Modeling and Optimization*, 1st ed. New York: Springer-Verlag, 2005.

[17] M. Westbrook, *The Electric and Hybrid Electric Car*. Warrendale, PA: Soc. Automotive Eng., 2001.

[18] R. Apter and M. Prathaler, "Regeneration of power in hybrid vehicles," in *Proc. IEEE 55th VTC Spring*, 2002, vol. 4, pp. 2063–2069.

[19] D. Linden and T. B. Reddy, *Batteries Handbook*, 3rd ed. New York: McGraw-Hill, 2002.

[20] K. Kawashima, T. Uchida, and Y. Hori, "Development of a novel ultra-capacitor electric vehicle and methods to cope with voltage variation," in *Proc. IEEE VPPC*, 2009, pp. 724–729.

[21] B. Blunier, M. G. Simões, and A. Miraoui, "Fuzzy logic controller development of a hybrid fuel cell-battery auxiliary power unit for remote applications," in *Conf. Rec. 9th IEEE Industry Applications Soc. Annu. Meeting*, Nov. 2010, pp. 1–6.

Alexandre Ravey (S'09) received the M.S. degree in electrical engineering in 2009 from the University of Technology of Belfort Montbéliard, Belfort, France, where he is currently working toward the Ph.D. degree.

His research interests include energy management of electric and hybrid vehicles.

Nicolas Watrin (S'10) received the M.S. degree in electrical engineering in 2009 from the University of Technology of Belfort-Montbéliard, Belfort, France, where he is currently working toward Ph.D. degree in association with Segula Technologie Automotive.

His current research interests include multiphysical hybrid vehicle component modeling and hybrid system sizing.

Benjamin Blunier (S'07–M'08) received the M.S. degree in science engineering from the University of Technology of Belfort-Monbteliard (UTBM), Belfort, France, in 2004.

Since 2008, he has been a Professor with UTBM. He is the author of the first textbook in French about fuel cells, i.e., *Pile à combustible: principes, technologies modélisation et application* (*Fuel cells: basic principles, technologies, modeling and applications*, published by Ellipses-Technosup, February 2007). His current research interests include electric and hybrid vehicles, fuel cells and, in particular, their modeling and air management.

David Bouquain received the Master's degree in electrical engineering from Franche-Comté University, Besançon, France, in 1999 and the Ph.D. degree in electrical engineering from the University of Technology of Belfort-Monbteliard (UTBM), Belfort, France, in 2008.

From 2000 to 2002, he was an Engineer with the Laboratoire de Recherche en Électronique, Électrotechnique et Systèmes (L2ES) Laboratory. He worked on a prototype of a hybrid truck for the French army. Since September 2002, he has been a Teacher and Researcher with the UTBM. He is currently an Associate Professor with the Systems and Transports Laboratory (SeT), UTBM, working on energy management of electric and hybrid vehicles and fuel cell systems.

Abdellatif Miraoui (M'07–SM'09) was born in Morocco in 1962. He received the M.Sc. degree from Haute Alsace University, Colmar-Mulhouse, France, in 1988 and the Ph.D. degree and the Habilitation to Supervise Research from Franche-Comte University, Besancon, France, in 1992 and 1999, respectively.

He has been a Full Professor of electrical engineering (electrical machines and energy) with the University of Technology of Belfort-Montbéliard (UTBM), Belfort, France, since 2000. He is the Vice President–Research Affairs of UTBM. He was the Director of the Department of Electrical Engineering, UTBM, from 2001 to 2009; Head of the "Energy Conversion and Command" Research Team (38 researchers on 2007); and Editor of the *International Journal on Electrical Engineering Transportation*. He is the author of more than 60 journal and 80 international conference proceeding papers. He is the author of the first textbook in French about fuel cells, entitled *Pile à combustible: principes, technologies modélization et applications* (published by Ellipses-Technosup, February 2007). His research interests include fuel cell energy, energy management (ultracapacitors, batteries, etc.) in transportation, design and optimization of permanent magnet synchronous motor (PMSM), and electrical propulsion/traction.

Prof. Miraoui is a member of several international journal and conference committees. He is a member of the IEEE Power Electronics, Industrial Electronics, and IEEE Vehicular Technology Societies. He is a Doctor Honoris Causa of Cluj-Napoca Technical University, Romania. He was the recipient of high distinction from the French Higher Education Ministry "Chevalier dans l'Ordre des Palmes Académiques" in 2007 and was also distinguished as Honorary Professor of the University of Brasov, Brasov, Romania.